

# Edge and Identity Preserving Network for Face Super-Resolution

Jonghyun Kim, Gen Li, Inyong Yun, Cheolkon Jung, and, Joongkyu Kim

**Abstract**—Face super-resolution has become an indispensable part in security problems such as video surveillance and identification system, but the distortion in facial components is a main obstacle to overcoming the problems. To alleviate it, most state-of-the-arts have utilized facial priors by using deep networks. These methods require extra labels, longer training time, and larger computation memory. Thus, we propose a novel Edge and Identity Preserving Network for Face Super-Resolution Network, named as EIPNet, which minimizes the distortion by utilizing a lightweight edge block and identity information. Specifically, the edge block extracts perceptual edge information and concatenates it to original feature maps in multiple scales. This structure progressively provides edge information in reconstruction procedure to aggregate local and global structural information. Moreover, we define an identity loss function to preserve identification of super-resolved images. The identity loss function compares feature distributions between super-resolved images and target images to solve unlabeled classification problem. In addition, we propose a Luminance-Chrominance Error (LCE) to expand usage of image representation domain. The LCE method not only reduces the dependency of color information by dividing brightness and color components but also facilitates our network to reflect differences between Super-Resolution (SR) and High-Resolution (HR) images in multiple domains (RGB and YUV). The proposed methods facilitate our super-resolution network to elaborately restore facial components and generate enhanced  $8\times$  scaled super-resolution images with a lightweight network structure. Furthermore, our network can generate a  $128 \times 128$  super-resolved image with 215 fps on a GTX 1080Ti GPU. Extensive experimental results demonstrate that our network qualitatively and quantitatively outperforms state-of-the-art methods on two challenging datasets: CelebA and VGGFace2.

**Index Terms**—Super-resolution, Face hallucination, Edge block, Identity loss, Image enhancement.

## I. INTRODUCTION

**F**ACE super-resolution is a challenging problem in computer vision, which requires reconstruction of extreme low-resolution images into high-resolution images. A main goal of the face super-resolution is to recognize human's identities, but it is difficult to restore high-frequency details in facial regions. For example, in an upscaling process from

Jonghyun Kim, Gen Li and Joongkyu Kim (corresponding author) are with the Department of Electronic, Electrical and Computer Engineering, Sungkyunkwan University, Suwon 16419, Republic of Korea e-mail: jkkim@skku.edu

Inyong Yun is with Hana Institute of Technology, Seoul 06133, Republic of Korea e-mail: iyyun@hanafn.com

Cheolkon Jung (corresponding author) are with the School of Electronic Engineering, Xidian University, Xian, Shaanxi 710071, China e-mail: zhengzk@xidian.edu.cn

This work was conducted when Jonghyun Kim visited Xidian University as a co-operating researcher.

Manuscript received Aug 18, 2020.

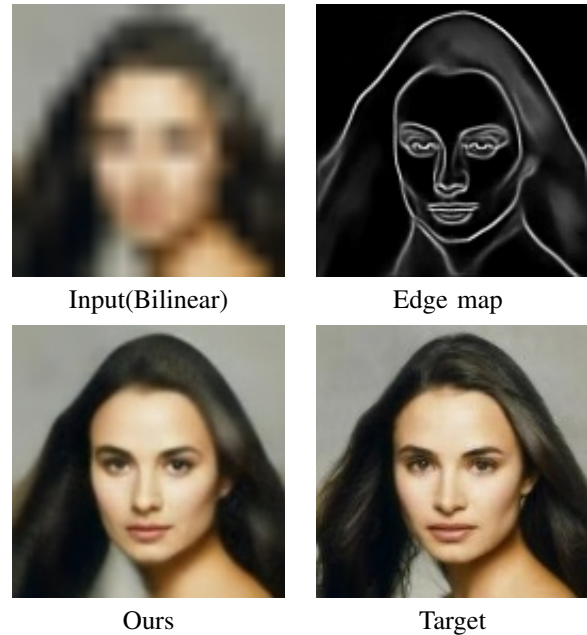


Fig. 1. Visualization of our super-resolution results on scale factor 8.

low-quality face images to high-resolution face images, the model suffers from distortion of facial components such as eyes, nose and mouth. Therefore, the elaborate restoration of the facial components is necessary for real-world applications, i.e., security, video surveillance system, face recognition and identification.

Previously, state-of-art methods [7], [8], [21] utilized edge information to mitigate endemic distortion problems in a super-resolution task. Such tendencies prove that the utilization of edges is an intuitive solution to improve super-resolved images. Specifically, these methods can be divided into two steps which consist of edge extraction and super-resolution conversion. Firstly, an edge network extracts edge information from low-resolution edge maps and images. Secondly, the extracted edge information is conveyed to a super-resolution network to compensate the high-frequency components, which leads to an increase in performance of the super-resolution methods. However, aforementioned methods employ a heavy convolutional network to generate edge maps and only consider the edge maps in a single scale.

On the other hand, current state-of-the-art methods [1]–[3], [5], [27] proposed a facial attention network to emphasize facial landmarks. The attention network highlights the facial components by multiplying attention masks or concatenating

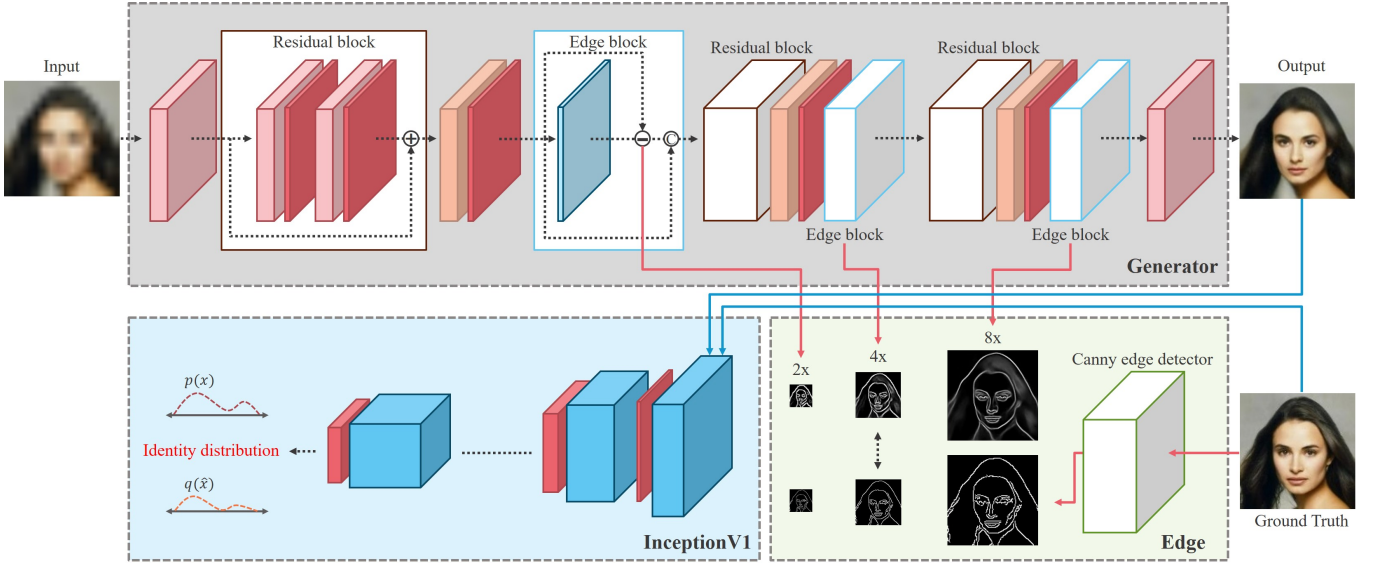


Fig. 2. Our proposed network structure. The residual block is comprised of two convolutional layers with ReLU [29]. The edge block is explained in Section III. We apply the InceptionV1 [28] network pretrained on VGGFace2 [23] for identity network.

attention maps on original feature maps. However, these methods require additional heavy networks (Encoder-Decoder network structure) to extract the facial landmarks. Although the landmarks positively militate the reconstruction of face structures, these methods lead to increase in computation cost and execution time. Moreover, the attention network needs extra labels for the facial landmarks to update its trainable parameters, but it is extremely difficult to obtain labels in the real-world.

In order to solve the aforementioned problems, we propose edge and identity preserving network for face super-resolution, called EIPNet, which elaborately reconstructs facial components in super-resolved face images by concatenating edge information to original feature maps as shown in Fig. 3. Compared to existing edge detection networks for super-resolution [7], [8], [21], the edge block is remarkably lightweight which comprises of a single convolutional layer and a single average pooling layer, but shows high-performance in detecting edge information. The edge block is embedded after each transposed convolutional block in multiple scales to provide structural information in each up-scaling process. Furthermore, we redefine an identity loss function to overcome unlabeled identity classification by comparing class-encoded vectors. An identity network extracts class-encoded vectors of super-resolved images and target images, and the identity loss function measures similarity between two vectors to distinguish these identities. We also propose Luminance-Chrominance Error (LCE) which simply converts RGB channels to YUV channels to independently utilize luminance and chrominance information as a loss function. The LCE method reflects distances between super-resolved images and high resolution images in multi domains, which provides plentiful information to our network. Therefore, our network generates precise super-resolution face images by intensively restoring facial details. The overall network structure is described in Fig. 2.

We evaluate the performance of our network on CelebA [9]

and VGGFace2 [23] datasets. For quantitative measurements, we use Peak Signal to Noise Ratio (PSNR) and Structural Similarity (SSIM) [11] as evaluation metrics. However, we do not use qualitative measurement, i.e., Mean-Opinion-Score (MOS) which is subjective and difficult to conduct on fair comparison. To deal with the lack of the comparison guideline, we suggest Facial Region PSNR (FR-PSNR) and Facial Region SSIM (FR-SSIM) to concentrate on facial details by cropping images with a face detection method [31]. The FR-PSNR and FR-SSIM exclude background and focus on the face region for exact and fair comparison.

Our main contributions can be described as follows:

- We propose the edge and identity preserving network for face super-resolution which overcomes distortion of facial components by providing the edge information and data distributions in the face super-resolution process. The edge block facilitates our proposed network to elaborately generate face super-resolution images. Furthermore, the identity loss compares class-encoded vectors to distinguish identities without related ground truth.
- We further propose the luminance-chrominance error (LCE) to align global shapes and colors. The LCE method converts RGB channels to YUV channels by using a conversion matrix, which separately generates luminance and chrominance information. We directly utilize these information to reflect distances between super-resolution face images and target images on our network with Mean-Square-Error (MSE) loss.
- To compensate for the lack of evaluation criterion, we introduce FR-PSNR and FR-SSIM to evaluate the restoration results of facial regions. The evaluation methods remove background components by cropping the output images with the face detection method, which emphasizes facial regions for comparison.

## II. RELATED WORK

### A. Edge information for Super-resolution

Intuitively, a single image can be divided into two components: low-frequency and high-frequency parts. The high-frequency component represents detailed information, called as edges, to construct structures of objects. Inspired by the property of edge, the state-of-the-arts [7], [8], [21] focused on reconstruction of the high-frequency component. In [8], three kinds of modules are proposed to generate super-resolution images. These modules are composed of SR network, Edge network, and Merge network. The SR network generates rough super-resolved images and the images are directly fed to the Edge network to extract edge maps. The outputs from the SR network and the Edge network are concatenated together. To reconstruct the high-frequency components in the outputs of the SR network, the Merge network combines the rough images and the edge maps. Similar with the proposed method in [8], the edge maps are utilized to enhance super-resolution images in [7]. A main contribution of [7] is that the super-resolution problem can be reformulated as an image inpainting task. Increasing the resolution of a given LR image requires recovery of pixel intensities between every two adjacent pixels. The missing pixels can be considered as missing regions of the inpainting task. To conduct the inpainting task, the edge maps sketch connection lines between the missing pixels in extended low-resolution images and a super-resolution network carries out image completion. Fang et al. [21] also employed an edge network to provide edge maps to a super-resolution network. In conclusion, these methods enhance super-resolved images by using edge information. However, a heavy network is unavoidable to extract edge information.

### B. Facial landmarks

In an upscaling process from low-quality face images to high-resolution face images, the distortion of facial components is the main obstacle. To address this problem, most state-of-the-art methods [1], [2], [5], [12], [13], [22] utilize facial landmarks or facial priors. FSRNet [1] proposes a prior estimation network to extract facial landmark heatmaps. Firstly, this method roughly generates a coarse super-resolution face image and extracts the prior information by using an Hour-Glass (HG) network [14]. Secondly, the prior heatmaps are concatenated with feature maps from an encoder network. Finally, feature maps are fed into a decoder network to generate super-resolution images. In a similar way, Yu et al. [5] also employs the HG network to detect facial landmarks and utilize the information. In [2], [13], a face alignment network (FAN) is proposed to compare facial heatmaps between super-resolution images and target images, but Kim et al. [2] constructs a single-scale network structure and trains the network to imitate output of the pre-trained HG network by using MSE loss. These tendencies prove that the HG network is an optimized estimator for extracting facial landmarks, but the HG network accompanies high computational cost and needs labels of facial landmarks. To overcome the dependence on facial landmarks, GWAInet [3] proposes an exemplar guiding method which provides a guiding face to refer its details

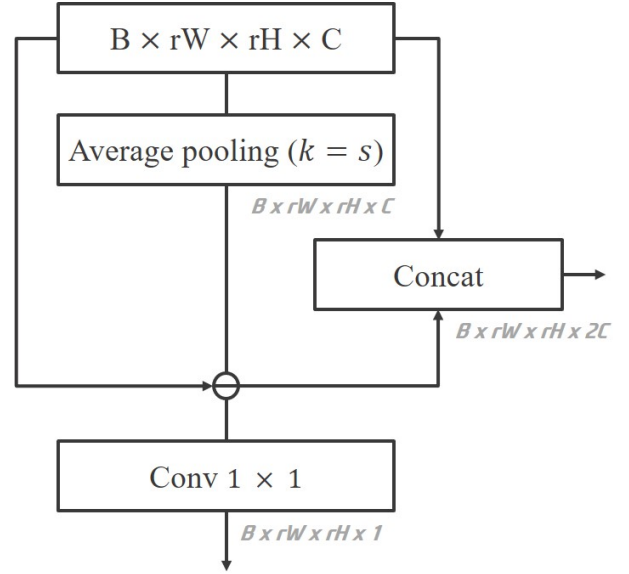


Fig. 3. Network structure of the proposed edge block.  $r$  is the scaling factor to consider multiple scales and  $s$  is the kernel size of the average pooling layer in each scale. The average pooling with padding imitates a median filter to generate smoothen feature maps.

and preserves the same identity in a restoration process. The method needs extra networks for warping the guiding image to input image and extracting feature maps from the warped image. The network shows comparable results with the restoration of the facial components. However, the network needs extra labels (e.g. guiding face images) to train the network and it is difficult to obtain the labels in the real-world.

## III. PROPOSED METHOD

### A. Edge Block

Edge information is utilized to enhance images in extensive areas such as super-resolution [7], [8], [21], image inpainting [24] and denoising tasks [25]. Without any doubt, edge information is a critical factor to not only elaborately reconstruct facial details from low-resolution face images but also solve an endemic problem of  $l_2$  distances loss which tends to generate smoothed images in the super-resolution. In detail, the edge information compensates missing parts in high-frequency components, such as edges of facial components and boundaries of face, to enhance the smoothed images. To extract and utilize edge information from features, we propose a lightweight edge block which is comprised of a single convolutional layer and a single average pooling layer as shown in Fig. 3. Firstly, the average pooling layer is same as a median filter with different kernel sizes ( $k = s$ ) in multiple scales to generate smoothed feature maps. Secondly, the edge block obtains high-frequency components by subtracting the smoothed feature maps from original feature maps. Finally, the subtracted feature maps are concatenated with original feature maps to convey the edge information to the next residual block. To update our edge block, a  $1 \times 1$  convolutional layer reduces the number of the subtracted feature maps to a single channel matched with edge

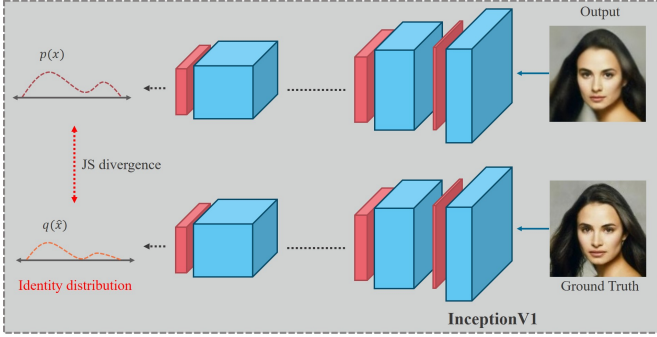


Fig. 4. Flow chart of the proposed identity loss. We adopt the InceptionV1 [28] network pretrained on VGGFace2 [23] to extract class-encoded vectors between output and ground truth images.

information of high-resolution input images which is generated by the canny edge detector [20] with thresholds of 100 and 255. The loss function for the edge block is defined as:

$$L_e = \frac{1}{r^2wh} \sum_{x=1}^{rw} \sum_{y=1}^{rh} \|C(I_{HR})(x, y) - E(I_{LR})(x, y)\|^2 \quad (1)$$

where  $E$  is the edge block,  $C$  is the canny edge detector,  $I_{HR}$  and  $I_{LR}$  are target face images and input low-resolution images, respectively. We consider edge information in multiple scales with scaling factor  $r$  which is set to be 1, 2, and 4.

### B. Identity Loss

Gottfried Wilhelm Leibniz, who was a German polymath and logician, mentioned no two leaves are alike in a forest of a hundred thousand trees. Also, no two identities are alike in the world. It means that the identity is an important criterion in terms of distinguishing each people. Even if some methods alleviate the distortion of facial details, it is not meaningful that super-resolved images do not have the same identity as their target images. Inspired by the concept, we propose a novel identity loss to minimize the distance of the identity as shown in Fig. 4. We use Kullback-Leibler (KL) divergence including cross-entropy to calculate the distance of two identities. The relationship between KL divergence and cross-entropy can be described as follows:

$$\begin{aligned} H_{p,q}(X) &= - \sum_{i=1}^N p(x_i) \log q(\hat{x}_i) \\ &= D_{KL}(p \parallel q) + H_p(X), \end{aligned} \quad (2)$$

where  $x$  and  $\hat{x}$  are a target image and a super-resolved image respectively,  $p$  and  $q$  are the probability distributions of the identity vector. In addition,  $D_{KL}(p \parallel q)$  can be summarized as  $\sum_{i=1}^N p(x_i) \log(\frac{p(x_i)}{q(\hat{x}_i)})$ . The cross-entropy function can be represented by the sum of KL divergence and entropy of distribution  $p$ . However,  $D_{KL}(p \parallel q)$  is non-symmetric which cause different results when a position of distribution  $p$  or  $q$  changed. To make a symmetric function, we use Jensen-Shannon (JS) divergence for the identity loss function which can be described as follows:

$$D_{JS} = \frac{1}{2} D_{KL}(p \parallel \frac{p+q}{2}) + \frac{1}{2} D_{KL}(q \parallel \frac{p+q}{2}). \quad (3)$$

Specifically, we extract 512-bins from target and super-resolved images to generate class-encoded vectors by using the InceptionV1 [28] network pretrained on VGGFace2 dataset [23]. The InceptionV1 model is suitable to extract identity properties as the model is trained to categorize the large-scale identities. Firstly, the class-encoded vectors are normalized to  $[0, 1]$  by a softmax function. Then, the JS divergence is directly applied to the normalized vectors to calculate the difference between two distributions. As a result, the final loss function of our identity concept is:

$$\begin{aligned} L_{id} &= \frac{1}{2} \sum_{i=1}^{512} \hat{p}(x_i) (\log \hat{p}(x_i) - \log(\frac{\hat{p}(x_i) + \hat{q}(\hat{x}_i)}{2})) \\ &\quad + \frac{1}{2} \sum_{i=1}^{512} \hat{q}(\hat{x}_i) (\log \hat{q}(\hat{x}_i) - \log(\frac{\hat{p}(x_i) + \hat{q}(\hat{x}_i)}{2})) \end{aligned} \quad (4)$$

where  $\hat{p}(x_i)$  and  $\hat{q}(\hat{x}_i)$  are the class-encoded vectors of ground truth and a super-resolved image respectively.

### C. Luminance-Chrominance Error

RGB domain has been adopted as the most popular image representation format among a lot of researches. In super-resolution areas, most state-of-the-art methods also utilized RGB domain with Mean-Square-Error loss to compare between their outputs and ground truth. However, based on experimental results in [26], YUV representation of an image has perceptually better quality than RGB. Furthermore, RGB channels contain blended information of luminance and chrominance components, which causes the redundancy to channel information, color distortion, and color shift.

To generate improved super-resolution images and alleviate above impacts, we propose luminance-chrominance error loss which not only converts RGB channels to YUV channels to split brightness and color components independently but also provides an additional criterion to update our network for the pixel-to-pixel task.

To be specific, we apply YUV conversion matrix to RGB channels to split luminance and chrominance parts as follows:

$$\begin{bmatrix} Y \\ U \\ V \end{bmatrix} = \begin{bmatrix} 0.299 & 0.587 & 0.114 \\ -0.14713 & -0.28886 & 0.436 \\ 0.615 & -0.51499 & -0.10001 \end{bmatrix} \begin{bmatrix} R \\ G \\ B \end{bmatrix} \quad (5)$$

where  $Y$  represents luminance information,  $U$  and  $V$  represent chrominance information.

We apply the conversion matrix to target images and generated images and compute the Mean-Square-Error (MSE) of the converted two sets of images as follows:

$$L_{lc} = \frac{1}{wh} \sum_{c=1}^{yuv} \sum_{x=1}^w \sum_{y=1}^h \|M(I_{HR})(x, y) - M(G(I_{LR}))(x, y)\|^2 \quad (6)$$

where  $M$  is the YUV conversion operator,  $G$  is our generator network,  $c$  is channels of YUV.

### D. Overall Loss Function

In addition to the loss functions discussed so far, we apply a couple of more loss functions as follows:

TABLE I. Configuration of the edge and identity preserving network for face super-resolution (EIPNet). All edge information is extracted after each transpose convolutional layer.

| Layer  | ReLU activation | Size of filter | Stride | Output channel | Output size ( $h \times w$ ) |
|--|-----------------|----------------|--------|----------------|------------------------------|
| <i>conv0</i>   | X               | $3 \times 3$   | 1      | 512            | $16 \times 16$               |
| <i>conv1_1</i>                                       | O               | $3 \times 3$   | 1      | 512            | $16 \times 16$               |
| <i>conv1_2</i>                                       | O               | $3 \times 3$   | 1      | 512            | $16 \times 16$               |
| <i>residual block1</i><br>( <i>conv0+conv1_2</i> )   | -               | -              | -      | 512            | $16 \times 16$               |
| <i>transpose conv1</i>                               | O               | $4 \times 4$   | 2      | 256            | $32 \times 32$               |
| <i>edge block1</i><br>( <i>t_conv1, edge1</i> )      | -               | -              | -      | 512            | $32 \times 32$               |
| <i>conv2_1</i>                                       | O               | $3 \times 3$   | 1      | 512            | $32 \times 32$               |
| <i>conv2_2</i>                                       | O               | $3 \times 3$   | 1      | 256            | $32 \times 32$               |
| <i>residual block2</i><br>( <i>t_conv1+conv2_2</i> ) | -               | -              | -      | 256            | $32 \times 32$               |
| <i>transpose conv2</i>                               | O               | $4 \times 4$   | 2      | 128            | $64 \times 64$               |
| <i>edge block2</i><br>( <i>t_conv2, edge2</i> )      | -               | -              | -      | 256            | $64 \times 64$               |
| <i>conv3_1</i>                                       | O               | $3 \times 3$   | 1      | 256            | $64 \times 64$               |
| <i>conv3_2</i>                                       | O               | $3 \times 3$   | 1      | 128            | $64 \times 64$               |
| <i>residual block3</i><br>( <i>t_conv2+conv3_2</i> ) | -               | -              | -      | 128            | $64 \times 64$               |
| <i>transpose conv3</i>                               | O               | $4 \times 4$   | 2      | 64             | $128 \times 128$             |
| <i>edge block3</i><br>( <i>t_conv3, edge3</i> )      | -               | -              | -      | 128            | $128 \times 128$             |
| <i>conv4</i>   | X               | $3 \times 3$   | 1      | 3              | $128 \times 128$             |

Context loss: We use the pixel-wise Mean-Square-Error (MSE) loss to minimize the distances between target images and generated images. The MSE loss is defined as:

$$L_{rgb} = \frac{1}{wh} \sum_{c=1}^{rgb} \sum_{x=1}^w \sum_{y=1}^h \|I_{HR}(x, y) - G(I_{LR})(x, y)\|^2 \quad (7)$$

where  $c$  is channels of RGB.

Adversarial loss: We use a Generative Adversarial Network (GAN) method to generate realistic super-resolved face images. The Adversarial loss is defined as:

$$L_{ad} = \mathbb{E}[\log D(I_{HR})] - \mathbb{E}[\log(1 - D(G(I_{LR})))] \quad (8)$$

where  $\mathbb{E}$  denotes the expectation of the probability distribution,  $D$  is the adversarial network.

Total loss: In our final network, we aggregate all loss functions. Thus, the total loss for training is described as:

$$L_{total} = L_{rgb} + \gamma L_e + L_{lc} + \alpha L_{id} + \beta L_{ad} \quad (9)$$

where  $\gamma$ ,  $\alpha$ ,  $\lambda$  and  $\beta$  are the weighting factors which are set empirically. Details of training manners will be mentioned in the next section.

### E. Network Architecture

The proposed network architecture in Fig. 2 is comprised of three residual blocks, three transposed convolutional blocks, and two convolutional layers in the first and last position of our network. Furthermore, three edge blocks are embedded after each transposed convolutional block. The overview on the configuration of our network is summarized in Table I. Specifically, the residual block consists of two  $3 \times 3$  convolutional layers with Rectifier Linear Unit (ReLU) as the activation function. The transposed convolutional block also use ReLU the same as the residual block. Each transposed block conducts  $2 \times$  upscaling and the final output is  $8 \times$  upscaled face images

from  $16 \times 16$  low-resolution input. After upsampling feature maps, the edge block is applied to obtain the sharp edge information on facial components. The edge block has a single  $1 \times 1$  convolutional layer and a single average pooling layer. After finishing all the processing, the last  $3 \times 3$  convolutional layer converts feature maps to RGB channels.

To generate realistic super-resolved images, we adopt the adversarial loss function. Concretely, our discriminator network is comprised of seven convolutional layers with Leaky ReLU and two fully-connected layers.

## IV. EXPERIMENTS

### A. Dataset

To evaluate our methods, we use two challenging datasets for face super-resolution: CelebA [9] and VGGFace2 [23]. The CelebA dataset is a large-scale face dataset with about 0.2 million images. The dataset provides aligned and unaligned face images. The aligned face images are cropped into square. We use both of face images to train and evaluate our model. For aligned face images, we use 162,770 images as a training set and 19,962 images as a test set. Furthermore, we also evaluate our model using unaligned face images. The unaligned dataset is comprised of 135,516 train images from a part of a test set in VGGFace2 dataset and 33,880 test images from remaining of the test set.

### B. Implementation Detail

To amplify the number of data images, we apply data augmentation as follows. We conduct center cropping with  $178 \times 178$  resolution and resizing  $128 \times 128$  for the CelebA dataset. For VGGFace2 dataset, we crop images with  $0.7 \times$  minimum resolution between height and width and resize  $128 \times 128$ . After the resizing process, we horizontally flip input images with a probability of 0.5 and rotate the images

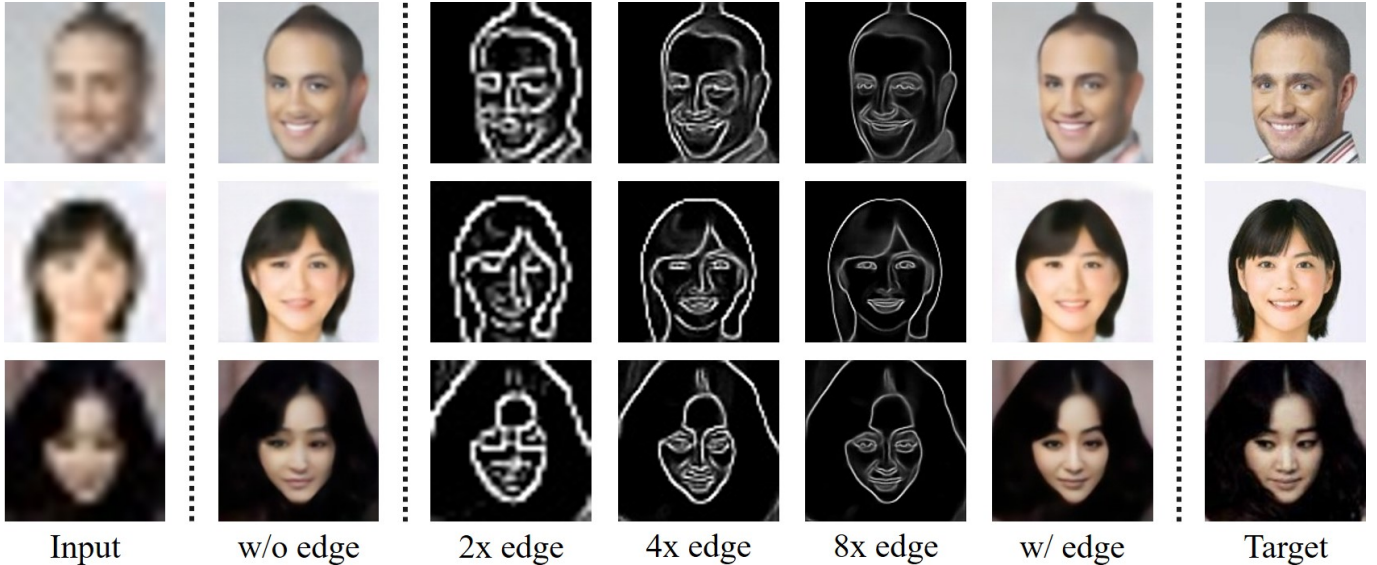


Fig. 5. Comparison of super-resolved images with/without the edge block. The input image has  $16 \times 16$  resolution and other outputs have  $128 \times 128$  resolution. The edge images are progressively extracted from each edge block. We resize the input and edge images to  $128 \times 128$  to intuitively show the figures.

by  $90^\circ$  and  $270^\circ$ . We progressively perform  $2 \times$  downscaling to generate  $8 \times$  downsampled low-resolution input images. As a test manner, we only use cropping and resizing by using the same resolution as that in training, and also apply  $8 \times$  downsampling for test images by using bilinear interpolation. For training, we use Adam optimizer [15] with  $\beta_1 = 0.9$ ,  $\beta_2 = 0.999$  and  $\epsilon = 1e - 8$  in the generator network, and  $\beta_1 = 0.5$  and  $\beta_2 = 0.9$  in the discriminator network. The learning rate is set to be  $1e - 4$ .

We train each dataset with above conditions except the adversarial loss parameter as  $\beta = 0$  until the iteration reaches 1.2M. Then, we train our networks with the adversarial loss function until the iteration reaches 1.32M. We conduct experiments on a single Tesla V100 GPU for training and a single GTX 1080ti for evaluation. All code is written and tested in Python with TensorFlow [16]. The code will be open in github.

### C. Evaluation metrics

We use Peak Signal to Noise Ratio (PSNR), Structural Similarity (SSIM), Facial Region PSNR (FR-PSNR), and Facial Region SSIM (FR-SSIM) to quantitatively evaluate our network. The FR-PSNR and FR-SSIM are suggested to replace subjective evaluation metric, i.e., Mean-Opinion-Score (MOS).

## V. ABLATION STUDY

### A. Edge block

Our super-resolution network employs the edge block in each upscaling process to preserve the high-frequency component. To verify that the proposed edge block preserves edges and boundaries of facial components, we conduct experiments with/without the edge block. Specifically, Fig. 5 shows that the visibility of eyes and mouth is improved by embedding the edge block compared to outputs of the baseline network

which use only  $L_{rgb}$  loss function. As can be seen from Fig. 5, the outputs with the edge block are clearly improved by comparing with the outputs without the edge block. Furthermore, the Fig. 5 shows that the edge block extracts sharp edge information of facial components in multiple scales by simply subtracting blurred feature maps from original feature maps. The subtracted feature maps are concatenated to original feature maps to complement high-frequency components. Such aggregation guides the EIPNet to elaborately reconstruct high-frequency components in facial components and generate enhanced super-resolved images.

The results prove that our edge network is effective in preserving edge information in the face super-resolution under a shallow and simple network. In order to reconstruct or enhance images using convolutional layer, the experimental results imply that our edge block can be simply applied to other domains with a marginal increase in learnable parameters.

### B. Identity loss

To prove the positive effect of the proposed identity loss, we evaluate super-resolved images with/without the identity loss in terms of preservation of identities. This experiment is conducted by a face recognition method [31] to compare identities between target and super-resolved images. The Fig. 6 is True and False cases of the experiment which shows that the outputs with the identity loss are a True case while the outputs without the identity loss are a False case. As can be seen from the figure, the identity loss reconstructs characteristics of facial details to make them perceptually similar to the target images.

In order to quantify the identity comparison, we adopt a conventional testing rule, where the accuracy is given as follows:

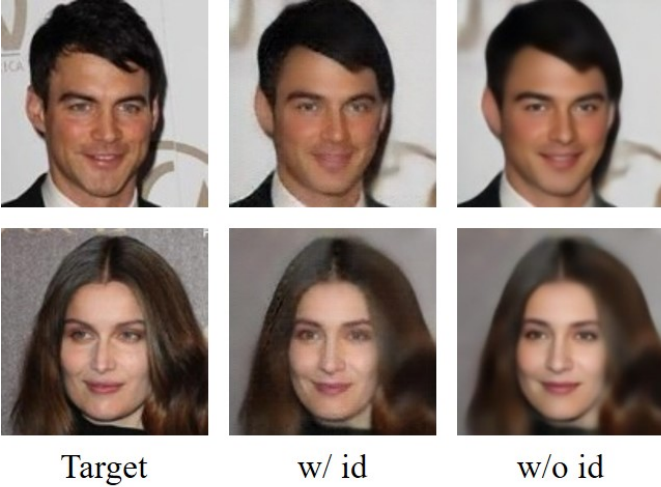


Fig. 6. Comparison of super-resolved images with/without the identity loss. The examples are True and False cases compared to identities of the target images.

TABLE II. Comparison with state-of-the-art methods in matching identities. This experiment is conducted according to the simple testing rule. The face recognition method [31] is applied to compare outputs of each method and ground truth.

| Method         |                   | Accuracy |
|----------------|-------------------|----------|
| IDN [33]       |                   | 46%      |
| Fu et al. [34] |                   | 57%      |
| Ours           | w/o identity loss | 58%      |
|                | w/ identity loss  | 64%      |

$$Acc = \frac{N_{CR}}{N_{ToT}} \times 100 \quad (10)$$

where  $N_{ToT}$  is the total number of test images and  $N_{CR}$  is the number of images correctly identified.

According to the testing rule, our method with the identity loss shows 64% accuracy which is 6% higher than the exclusion method. Furthermore, our method also outperforms other real-time super-resolution methods in terms of accuracy as can be seen from Table II. The experimental result proves that our identity loss is effective in preserving identities in upscaling process. Furthermore, the method alleviates endemic problems in the face super-resolution task such as blurring effect and artificiality.

### C. Luminance-Chrominance error

We evaluate the effect of luminance-chrominance error (LCE) in terms of quantitative evaluation metrics. The LCE shows an increase in all types of the evaluation metrics in Table III. However, it does not show perceptual improvement even if PSNR and SSIM are increased. It means that the luminance-chrominance loss conducts global fine-tune in each pixel by considering luminance and chrominance information separately.

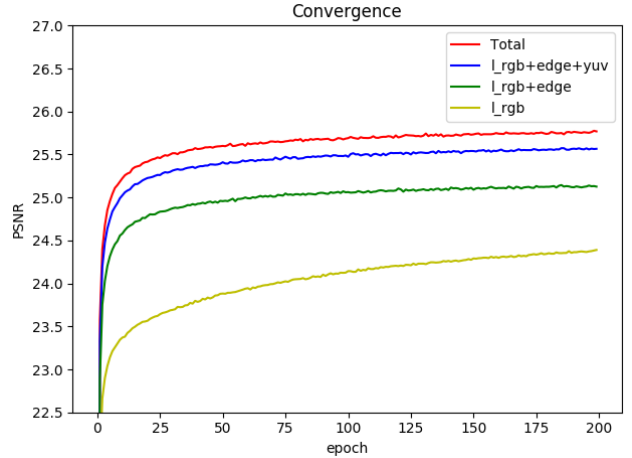


Fig. 7. Curves of the training procedure on CelebA for each loss function. We progressively add the proposed loss functions to  $L_{rgb}$ . The adversarial loss is excluded because a training method with the adversarial loss is different from other loss functions.

### D. Overview of contributions

In this paper, we propose three types of novel methods to enhance super-resolved images. To demonstrate that how our proposed methods affect our network in the training procedure, we attach Fig. 7 to represent curves of PSNR values per each epoch on the CelebA dataset for each loss function. These curves show that our proposed methods help our network to converge fast while the  $L_{rgb}$  loss gradually converges. It indicates that our methods are effective to rapidly reach a peak value in the training procedure.

To prove that our methods are also effective in the testing procedure, we attach Fig. 8 and Table III to show progressive improvements of super-resolved images depending on each loss function. In the testing procedure, our network takes  $16 \times 16$  low-resolution images as input and conducts the  $8 \times$  upscaling process as we mentioned in the implementation detail section.

According to the Fig. 8 and the Table III, our edge block shows a remarkable improvement in both qualitative and quantitative results by compensating for missing parts of the high-frequency component in upscaling layers. Specifically, the edge block alleviates blurring effect and shows a large improvement in PSNR and SSIM. On the other hand, other proposed methods do not show much difference in qualitative results while improving quantitative results. Finally, our method achieves 25.16 in PSNR and 0.7494 in SSIM. However, our network also suffers the perception-distortion trade-off as mentioned in [32]. The adversarial loss decreases the quantitative results even though the visual quality looks better.

## VI. COMPARISON WITH STATE-OF-THE-ART

Each face super-resolution method can be individually categorized by datasets, the size of images, and the ratio of scaling. We compare our method with four state-of-the-art

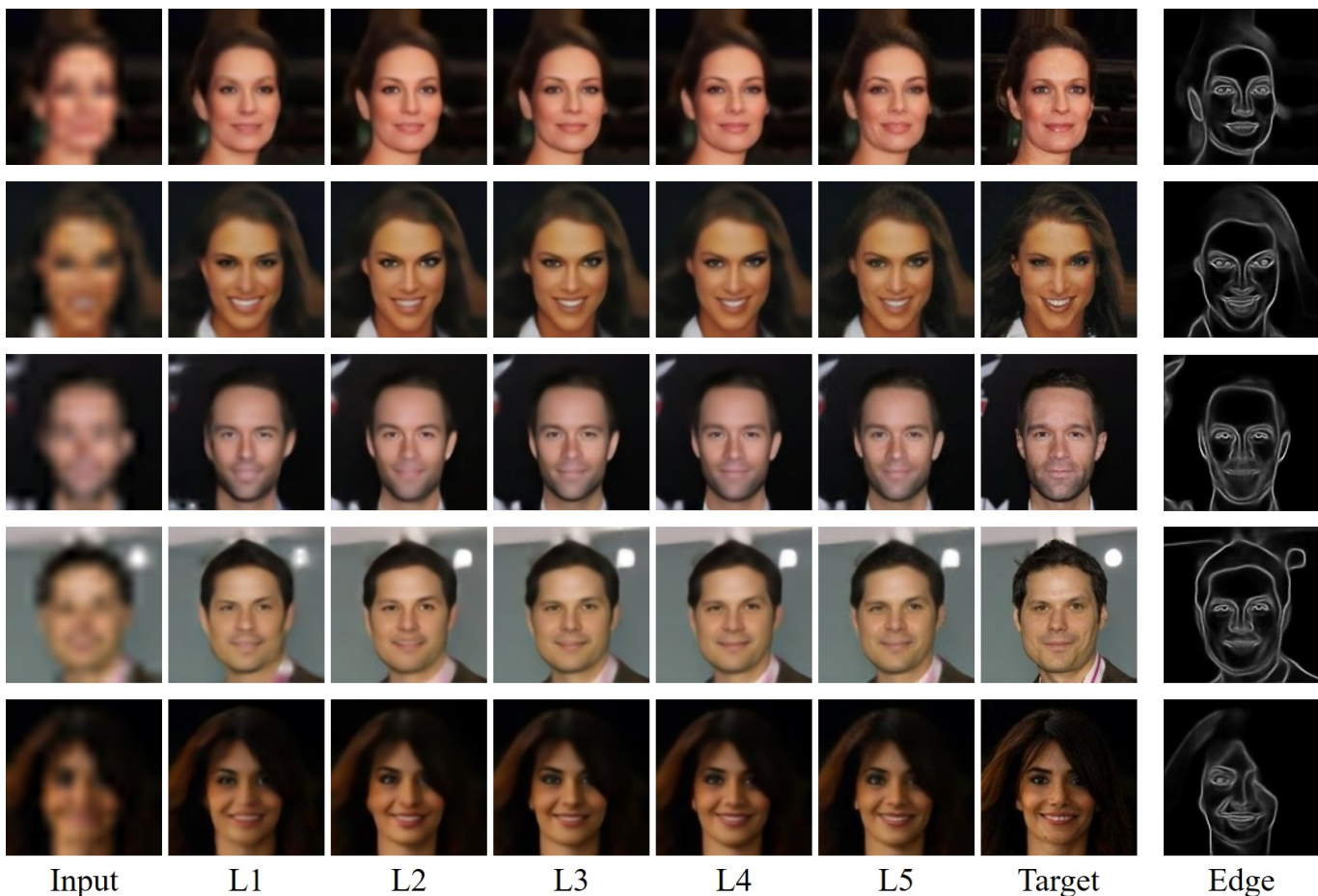


Fig. 8. Comparison of our outputs depending on loss functions. The input image has  $16 \times 16$  resolution and other outputs have  $128 \times 128$  resolution. The edge images are extracted from the third edge block. The  $L1$  utilizes only  $L_{rgb}$ . Starting from the  $L1$ , we progressively add  $L_e$ ,  $L_{lc}$ ,  $L_{id}$  and,  $L_{ad}$  to  $L5$ .

TABLE III. Comparison of the ablation study results in validation PSNR, FR-PSNR, SSIM, and FR-SSIM on CelebA dataset.

| Method                                     | PSNR  | FR-PSNR | SSIM   | FR-SSIM |
|--|-------|---------|--------|---------|
| Bicubic                                    | 18.45 | 18.12   | 0.4953 | 0.4565  |
| $L_{rgb}$                                  | 23.11 | 23.42   | 0.7070 | 0.7278  |
| $L_{rgb} + L_e$                            | 24.74 | 24.73   | 0.7339 | 0.7522  |
| $L_{rgb} + L_e + L_{lc}$                   | 25.05 | 25.15   | 0.7461 | 0.7699  |
| $L_{rgb} + L_e + L_{lc} + L_{id}$          | 25.16 | 25.31   | 0.7494 | 0.7745  |
| $L_{rgb} + L_e + L_{lc} + L_{id} + L_{ad}$ | 25.08 | 25.20   | 0.7429 | 0.7696  |

methods which are FSRGAN [1], Kim et al. [2], IDN [33], Fu et al. [34]. These methods have the similar experimental conditions to ours to quantitatively and qualitatively compare our results. Furthermore, we compare our proposed method with these state-of-the-arts in computational cost and the processing speed.

#### A. Quantitative and qualitative comparison

In order to validate the effectiveness of our proposed method, we compare our method with aforementioned state-of-the-art methods in terms of quantitative and qualitative measures. The Table IV shows quantitative results on different datasets. Experimental results shows that our proposed method achieves the best PSNR and SSIM performance among other

existing methods on both datasets regardless of GAN. Specifically, the PSNR and SSIM value of our proposed method without GAN are 0.75 dB and 0.0244 respectively higher than output of Fu et al., which shows the best performances among existing methods with a lightweight structure. Furthermore, our proposed method with GAN obtains comparable performance with PSNR-oriented methods such as IDN and Fu et al.. It indicates that our proposed method is able to preserve pixel-wise accuracy while increasing perceptual quality of the super-resolved images.

We visualize some examples of super-resolved images on both datasets as shown in Fig. 9. We can see that our proposed method restores correct facial details while other methods generates failed cases. The reason is that the edge block progressively reconstruct facial structures by concatenating the



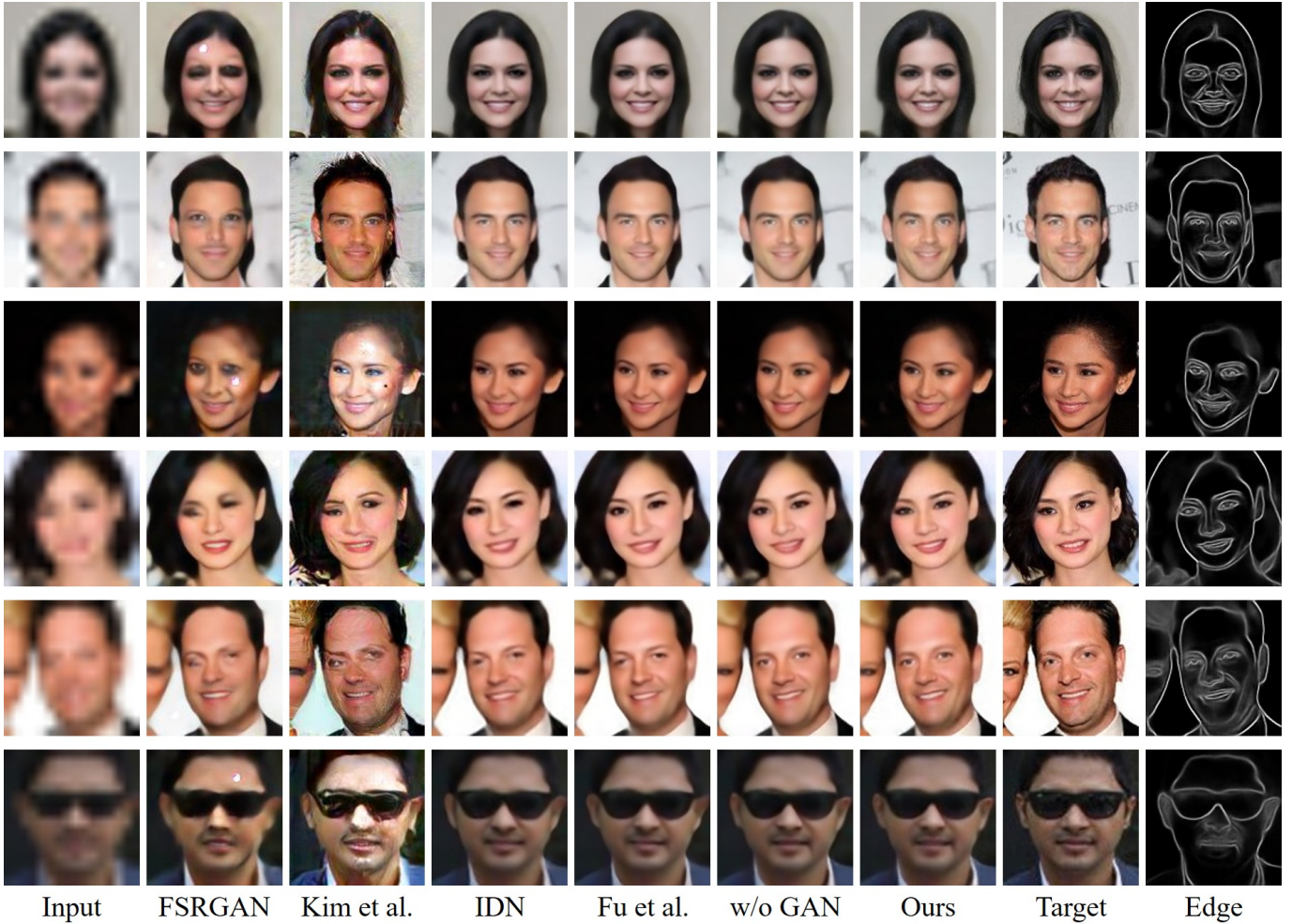


Fig. 9. Qualitative comparison with state-of-the-art methods. The size of input and output is the  $16 \times 16$  and  $128 \times 128$  respectively. From the first row to the third row, example images are from CelebA, others are from VGGFace2. In the last column, edge images are generated by our edge block. For the best view, please zoom in this figure.

TABLE IV. Quantitative comparison with state-of-the-art methods on CelebA and VGGFace2. To concentrate on facial regions, we use FR-PSNR and FR-SSIM criteria. For these criteria, we extract the facial regions from each super-resolved image by utilizing the face recognition method.

| Dataset  | Method         | PSNR  | FR-PSNR | SSIM   | FR-SSIM |
|----------|----------------|-------|---------|--------|---------|
| CelebA   | FSRGAN [1]     | 22.84 | 22.13   | 0.6665 | 0.6451  |
|          | Kim et al. [2] | 23.19 | 23.62   | 0.6798 | 0.7288  |
|          | IDN [33]       | 24.28 | 24.37   | 0.7170 | 0.7424  |
|          | Fu et al. [34] | 24.41 | 24.62   | 0.7250 | 0.7561  |
|          | w/o GAN        | 25.16 | 25.31   | 0.7494 | 0.7745  |
|          | Ours           | 25.08 | 25.20   | 0.7429 | 0.7696  |
| VGGFace2 | FSRGAN [1]     | 22.02 | 21.58   | 0.6463 | 0.6423  |
|          | Kim et al. [2] | 22.65 | 22.23   | 0.6699 | 0.6560  |
|          | IDN [33]       | 24.26 | 24.49   | 0.6969 | 0.6997  |
|          | Fu et al. [34] | 24.30 | 24.62   | 0.7017 | 0.7083  |
|          | w/o GAN        | 24.72 | 25.01   | 0.7148 | 0.7201  |
|          | Ours           | 24.56 | 24.83   | 0.7066 | 0.7138  |

high-frequency component to original feature maps. Thus, our proposed method performs better in restoring facial structures and alleviating blurring effect. Furthermore, our method with GAN generates more realistic images while other methods generates distortions or non-realistic images. Consequently, the qualitative comparison proves that our proposed method

is an influential network to generate improved images.

### B. Computational comparison

Since each method employ various devices, we conduct the computational and speed experiments with a single GTX 1080Ti GPU on the Tensorflow platform for fair comparison

TABLE V. Computational and speed comparison with state-of-the-art methods. All the runtime is computed with a single GTX 1080Ti on the Tensorflow platform.

| Method     | Parameter    | GMACs       | FPS        | PSNR         | SSIM          |
|------------|--------------|-------------|------------|--------------|---------------|
| FSRGAN     | 2.15M        | 15.79       | 62         | 22.84        | 0.6665        |
| Kim et al. | 6.83M        | 3.36        | <b>317</b> | 23.19        | 0.6798        |
| IDN        | <b>0.68M</b> | <b>0.17</b> | 92         | 24.28        | 0.7170        |
| Fu et al.  | 2.96M        | 5.54        | 213        | 24.41        | 0.7250        |
| Ours       | 11.91M       | 10.16       | 215        | <b>25.08</b> | <b>0.7429</b> |

of the speed. Table V represents computational and the speed comparison with state-of-the-art methods on CelebA dataset. Kim et al. [2] outperforms existing methods with big difference while quantitative results are lower than others. However, our proposed method shows the best results in the pixel-oriented criteria with 215 FPS. Fu et al. [34] is one of the fastest real-time method for super-resolution, and our method is a slightly faster than it. The experimental results represents that our proposed method is able to show the competitive speed while maintaining high performance.

## VII. CONCLUSION

In this paper, we proposed Edge and Identity Preserving Network for Face Super-Resolution. The edge block compensates missing parts in the high-frequency components to mitigate blurring effect and the luminance-chrominance error conducts global fine-tune to improve pixel-wise accuracy. Moreover, the identity loss reconstructs super-resolved images while preserving these personal identities. Based on these proposed methods, the EIPNet is able to generate enhanced super-resolved images while reconstructing the high-frequency components and personal identities. According to the extensive experimental result and ablation studies, we demonstrate the effectiveness of our method. Overall, our network shows competitive results in pixel-wise accuracy and inference speed compared with the state-of-the-art methods. However, our network yet achieves the lowest computational cost and the highest speed. We will keep improving our network to solve these problems while increasing perceptual quality of the super-resolved images.

## ACKNOWLEDGMENT

This research was supported by the MSIT(Ministry of Science, ICT), Korea, under the High-Potential Individuals Global Training Program(2019-0-01609) supervised by the IITP(Institute for Information Communications Technology Planning Evaluation); the National Research Foundation of Korea(NRF) grant funded by the Korea government (MSIT) (No. 2020R1A2C1012159).

## REFERENCES

- [1] CHEN, Yu, et al. Fsrnet: End-to-end learning face super-resolution with facial priors. In: Proceedings of the IEEE Conference on Computer Vision and Pattern Recognition. 2018. p. 2492-2501.
- [2] KIM, Deokyun, et al. Progressive Face Super-Resolution via Attention to Facial Landmark. arXiv preprint arXiv:1908.08239, 2019.
- [3] DOGAN, Berk; GU, Shuhang; TIMOFTE, Radu. Exemplar Guided Face Image Super-Resolution without Facial Landmarks. In: Proceedings of the IEEE Conference on Computer Vision and Pattern Recognition Workshops. 2019. p. 0-0.
- [4] GOODFELLOW, Ian, et al. Generative adversarial nets. In: Advances in neural information processing systems. 2014. p. 2672-2680.
- [5] YU, Xin, et al. Face super-resolution guided by facial component heatmaps. In: Proceedings of the European Conference on Computer Vision (ECCV). 2018. p. 217-233.
- [6] GULRAJANI, Ishaan, et al. Improved training of wasserstein gans. In: Advances in neural information processing systems. 2017. p. 5767-5777.
- [7] NAZERI, Kamyar; THASARATHAN, Harrish; EBRAHIMI, Mehran. Edge-Informed Single Image Super-Resolution. In: Proceedings of the IEEE International Conference on Computer Vision Workshops. 2019. p. 0-0.
- [8] KIM, Kwanyoung; CHUN, Se Young. SREdgeNet: Edge Enhanced Single Image Super Resolution using Dense Edge Detection Network and Feature Merge Network. arXiv preprint arXiv:1812.07174, 2018.
- [9] LIU, Ziwei, et al. Large-scale celebfaces attributes (celeba) dataset. Retrieved August, 2018, 15: 2018.
- [10] KOESTINGER, Martin, et al. Annotated facial landmarks in the wild: A large-scale, real-world database for facial landmark localization. In: 2011 IEEE international conference on computer vision workshops (ICCV workshops). IEEE, 2011. p. 2144-2151.
- [11] WANG, Zhou, et al. Image quality assessment: from error visibility to structural similarity. IEEE transactions on image processing, 2004, 13.4: 600-612.
- [12] KALAROT, Ratheesh; LI, Tao; PORIKLI, Fatih. Component Attention Guided Face Super-Resolution Network: CAGFace. arXiv preprint arXiv:1910.08761, 2019.
- [13] BULAT, Adrian; TZIMIROPOULOS, Georgios. Super-FAN: Integrated facial landmark localization and super-resolution of real-world low resolution faces in arbitrary poses with GANs. In: Proceedings of the IEEE Conference on Computer Vision and Pattern Recognition. 2018. p. 109-117.
- [14] NEWELL, Alejandro; YANG, Kaiyu; DENG, Jia. Stacked hourglass networks for human pose estimation. In: European conference on computer vision. Springer, Cham, 2016. p. 483-499.
- [15] KINGMA, Diederik P.; BA, Jimmy. Adam: A method for stochastic optimization. arXiv preprint arXiv:1412.6980, 2014.
- [16] ABADI, Martn, et al. Tensorflow: A system for large-scale machine learning. In: 12th USENIX Symposium on Operating Systems Design and Implementation (OSDI 16). 2016. p. 265-283.
- [17] IOFFE, Sergey; SZEGEDY, Christian. Batch normalization: Accelerating deep network training by reducing internal covariate shift. arXiv preprint arXiv:1502.03167, 2015.
- [18] SIMONYAN, Karen; ZISSERMAN, Andrew. Very deep convolutional networks for large-scale image recognition. arXiv preprint arXiv:1409.1556, 2014.
- [19] DENG, Jia, et al. Imagenet: A large-scale hierarchical image database. In: 2009 IEEE conference on computer vision and pattern recognition. Ieee, 2009. p. 248-255.
- [20] CANNY, John. A computational approach to edge detection. IEEE Transactions on pattern analysis and machine intelligence, 1986, 6: 679-698.
- [21] FANG, Faming; LI, Juncheng; ZENG, Tiejong. Soft-Edge Assisted Network for Single Image Super-Resolution. IEEE Transactions on Image Processing, 2020, 29: 4656-4668.
- [22] YIN, Yu, et al. Joint Super-Resolution and Alignment of Tiny Faces. arXiv preprint arXiv:1911.08566, 2019.
- [23] CAO, Qiong, et al. Vggface2: A dataset for recognising faces across pose and age. In: 2018 13th IEEE International Conference on Automatic Face & Gesture Recognition (FG 2018). IEEE, 2018. p. 67-74.
- [24] NAZERI, Kamyar, et al. Edgeconnect: Generative image inpainting with adversarial edge learning. arXiv preprint arXiv:1901.00212, 2019.
- [25] CHEN, Xi, et al. Image denoising via deep network based on edge enhancement. Journal of Ambient Intelligence and Humanized Computing, 2018, 1-11.
- [26] PODPORA, Michal; KORBAS, Grzegorz Pawel; KAWALA-JANIK, Aleksandra. YUV vs RGB-Choosing a Color Space for Human-Machine Interaction. FedCSIS Position Papers, 2014, 18: 29-34.
- [27] YIN, Yu, et al. Joint Super-Resolution and Alignment of Tiny Faces. arXiv preprint arXiv:1911.08566, 2019.
- [28] SZEGEDY, Christian, et al. Going deeper with convolutions. In: Proceedings of the IEEE conference on computer vision and pattern recognition. 2015. p. 1-9.

- [29] NAIR, Vinod; HINTON, Geoffrey E. Rectified linear units improve restricted boltzmann machines. In: Proceedings of the 27th international conference on machine learning (ICML-10). 2010. p. 807-814.
- [30] YU, Xin, et al. Super-resolving very low-resolution face images with supplementary attributes. In: Proceedings of the IEEE Conference on Computer Vision and Pattern Recognition. 2018. p. 908-917.
- [31] [https://github.com/ageitgey/face\\_recognition](https://github.com/ageitgey/face_recognition)
- [32] BLAU, Yochai; MICHAELI, Tomer. The perception-distortion tradeoff. In: Proceedings of the IEEE Conference on Computer Vision and Pattern Recognition. 2018. p. 6228-6237.
- [33] HUI, Zheng; WANG, Xiumei; GAO, Xinbo. Fast and accurate single image super-resolution via information distillation network. In: Proceedings of the IEEE conference on computer vision and pattern recognition. 2018. p. 723-731.
- [34] FU, Shipeng, et al. A Real-Time Super-Resolution Method Based on Convolutional Neural Networks. Circuits, Systems, and Signal Processing, 2020, 39.2: 805-817.



**Jonghyun Kim** received the B.S. degree in Electronic and Computer Engineering from Chonnam National University at Gwang-Ju, Republic of Korea, in 2018. He is currently pursuing his Ph.D. degree in Electronic, Electrical and Computer Engineering at Sungkyunkwan University, Republic of Korea. His research interests include image and video processing, video analysis, machine learning, super-resolution, image translation.



**Gen Li** received the B.S. degree in Electronic and Information Engineering from Xidian University, Xi'an, China, in 2018. He is currently pursuing the M.S. degree in Electronic, Electrical and Computer Engineering at SungKyunKwan University, Suwon, South Korea. His research interests include computer vision, deep learning, object detection, and semantic segmentation.



**Inyong Yun** received the B.S. degree in ocean engineering from Jeju National University, Republic of Korea, in 2010, and the Ph.D. degree in electronic engineering at Sungkyunkwan University, Republic of Korea. He is currently working for Hana Institute of Technology, Republic of Korea as a senior researcher. His main research interests include image and video processing, computer vision and machine learning.



**Cheolkon Jung** received the B.S., M.S., and Ph.D. degrees in electronic engineering from Sungkyunkwan University, Republic of Korea, in 1995, 1997, and 2002, respectively. He was with the Samsung Advanced Institute of Technology (Samsung Electronics), Republic of Korea, as a Research Staff Member from 2002 to 2007. He was a Research Professor in the School of Information and Communication Engineering at Sungkyunkwan University, Republic of Korea, from 2007 to 2009. Since 2009, he has been with the School of Electronic Engineering at Xidian University, China, where he is currently a Full Professor and the Director of the Xidian Media Lab. His main research interests include image and video processing, computer vision, pattern recognition, machine learning, computational photography, video coding, virtual reality, information fusion, multimedia content analysis and management, and 3DTV.



**Joongkyu Kim** received the B.S. and M.S. degrees in electronic engineering from Seoul National University, Korea, in 1980 and 1982, respectively, and the Ph.D. degree in electrical engineering and computer science from the University of Michigan, Ann Arbor, in 1989. From 1990 to 1991, he worked for Samsung Electronics, Korea, as a project leader working on the development of the tactical air surveillance radar TARS system. Since 1992, he has been with the School of Information and Communication Engineering at Sungkyunkwan University, Korea, where he is currently a Professor. His research interests lie in the areas of signal processing, detection and estimation of noise canceling, biomedical signal/image processing, and application of time-frequency distribution for non-stationary signal analysis.